Chemical Science

ROYAL SOCIETY OF CHEMISTRY

EDGE ARTICLE

View Article Online
View Journal | View Issue

Cite this: *Chem. Sci.*, 2024, **15**, 20365

All publication charges for this article have been paid for by the Royal Society of Chemistry

Received 10th September 2024
Accepted 12th November 2024

DOI: 10.1039/d4sc06110a

rsc.li/chemical-science

An efficient all-visible light-activated photoswitch based on diarylethenes and CdS quantum dots†

Kezhou Chen,[ab] Jiayi Liu,[ab] Joakim Andréasson,[c] Bo Albinsson,[*c] Tiegen Liu*[ab] and Lili Hou[*abc]

All-visible light-activated diarylethene (DAE) photoswitches are highly attractive for applications in smart photoresponsive materials. The photocyclization of DAE *via* the low-lying excited triplet state through triplet energy transfer (TET) from a sensitizer has been proven to be an effective approach for the realization of this scheme. However, the TET process is sensitive to oxygen and typically requires more than one sensitizer per photoswitch to facilitate sensitized photocyclization. Herein, we present a bi-component system comprising carboxylic acid-functionalized DAEs and CdS quantum dots (QDs) to achieve all-visible light-activated photoswitching. Due to the large surface area-to-volume ratio of CdS QDs and surface anchored DAEs, one CdS QD can activate at least 18 DAE molecules in the solution without oxygen exclusion. The efficiency of photocyclization of DAEs under visible light irradiation through energy transfer from CdS QDs is nearly comparable to that of direct UV light irradiation. Moreover, our strategy is adaptable for solid-state applications in the presence of air, enabling reversible writing and erasing of color and patterns by adjusting irradiation wavelengths in the visible region.

Introduction

Photoresponsive materials, possessing the ability to react or respond to light stimuli, have been widely applied in various fields such as biological imaging, smart devices, and energy storage.[1–3] Among these materials, photochromic molecules, also referred to as molecular photoswitches, have attracted extensive research interest due to their capability of reversibly converting between two states with distinct physical and chemical properties upon irradiation at different light wavelengths.4–7 Diarylethene (DAE) is one of the most commonly used photoswitches, whose ring-open and ring-closed isomers can be reversibly and repeatedly interconverted into each other upon alternating irradiation with UV and visible light.[8,9] DAEs exhibit excellent properties, such as high coloration/decoloration contrast and thermal stability, making them ideal photoresponsive materials for sensing, bioimaging, and memory applications.[10–14] Photoluminescence switching materials composed of quantum dots (QDs) and DAE have been widely researched.[15–17] However, most DAE photoswitches require UV light to trigger the closing reaction, which can result in the formation of by-products during photoisomerization and thus limit the photostability.[18] Moreover, UV light has a very poor penetration depth and causes cell damage, which presents obstacles in future biological applications. Therefore, it is highly desired to develop all-visible light-activated DAEs.[19]

One approach to achieving this goal is through a triplet energy transfer (TET) reaction from a sensitizer, by which the photocyclization of DAEs (conversion from the ring-open to the closed isomer) occurs in the triplet excited state (T_1).[20] The lower energy of T_1 compared to the singlet excited state (S_1) enables the photocyclization of DAEs using longer excitation wavelengths, and the absence of by-product formation in the T_1 state can improve the photostability of DAEs.[21–26] Typical metal complexes (Ru, Re, Os, Pt, *etc.*) and organic triplet sensitizers (biacetyl, perylene, xanthone, *etc.*) have been used to activate different DAE derivatives upon visible light irradiation through intersystem crossing (ISC) and subsequent TET to DAE.[26–32] The strategies to introduce a triplet sensitizer can involve direct mixing or covalent bonding. As the commonly used sensitizers feature a large singlet–triplet energy gap (ΔE_{ST}) and weak light absorption in the visible region (low molar absorption coefficients), a large excess (up to 250-fold) of the organic sensitizer is required to induce efficient photoswitching *via* direct mixing.[21] Zhang and co-workers introduced thermally activated delayed fluorescence (TADF) materials, 1,2-bis(carbazol-9-yl)-4,5-dicyanobenzene (2CzPN) and 1,2,3,5-tetrakis(carbazol-9-yl)-4,6-dicyanobenzene (4CzIPN), as sensitizers to achieve efficient visible-light driven isomerization of DAEs.[21] The small ΔE_{ST} of

[a]*School of Precision Instrument and Opto-Electronics Engineering, Tianjin University, Tianjin 300072, China. E-mail: lilihou@tju.edu.cn*

[b]*Key Laboratory of Opto-electronics Information Technology (Tianjin University), Tianjin 300072, China*

[c]*Department of Chemistry and Chemical Engineering, Chalmers University of Technology, Gothenburg 412 96, Sweden*

† Electronic supplementary information (ESI) available. See DOI: https://doi.org/10.1039/d4sc06110a

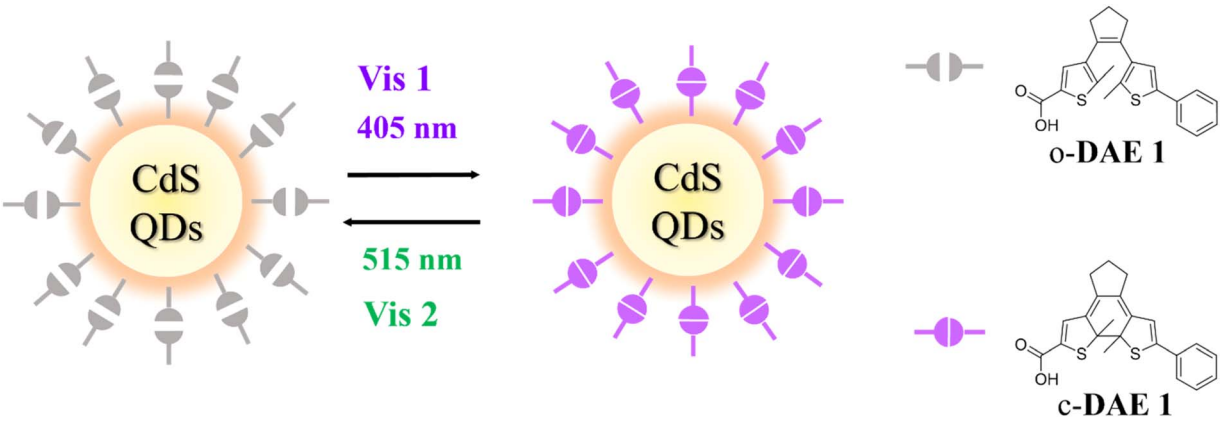

Scheme 1 Schematic illustration of all-visible light activated modulation of the CdS QDs and carboxylated **DAE 1** in the open and closed forms.

TADF molecules allows for reducing the ratio between the sensitizer and DAE molecules to 3 : 1. Recently, our group and others introduced colloidal QDs, specifically CdS and perovskite QDs, as sensitizers to achieve all-visible light-activated DAEs.[33,34] The amount of sensitizing QDs required can be significantly reduced due to the narrow ΔE_{ST}, high molar absorption coefficients, and large surface area-to-volume ratio of QDs. However, a mediator is required to relay the TET from QDs to DAEs. It should be noted that previously, when considering the ratio between the molecular mediator and DAE, a minimum ratio of 3 : 1 was required. Covalent linkage between organic molecules and DAEs is also a significant breakthrough in all-visible light-activated DAEs.[31,35–40] By extending the π-conjugation or linking sensitizers, visible light was able to drive the photo-induced ring-closing process of DAE. However, this approach involves complicated synthesis procedures, which reduce the overall appeal. Moreover, most of these triplet sensitized approaches are sensitive to the presence of oxygen due to the inherent characteristics of the long-lived triplet states involved.

Herein, we have developed an efficient all-visible light-activated photoswitchable system composed of CdS QDs and carboxylated DAEs (**DAE 1**), as shown in Scheme 1. In the solution, **DAE 1** can dynamically anchor to the surface of CdS QDs through coordination bonding of its carboxylic acid functional groups during collisions as proved by Fourier-transform Infrared (FTIR) spectra (details in the ESI†), resulting in a photoswitchable system where a single CdS QD can efficiently activate at least 18 DAE molecules upon visible light irradiation. Importantly, our all-visible light activated photoswitchable system can be operated under air equilibrated conditions in the presence of oxygen. Moreover, when casting CdS QDs and **DAE 1** on paper in the solid state, different patterns can be written and erased using light at 405 nm and 515 nm as external stimuli.

Results and discussion

Photochromic behaviour

CdS QDs and **DAE 1** were synthesized according to previous reports.[16,41,42] The Transmission Electron Microscope (TEM) image of CdS QDs reveals a uniform spherical morphology with an average diameter of 3.5–4 nm (Fig. S1a†). The crystallinity of CdS QDs has been investigated by conventional X-ray diffraction (XRD) (see Fig. S1b†). The diffraction peaks of 2θ appearing at ~26.57° and 43.74° correspond to the (111) and (220) crystal planes of CdS QDs,[41] consistent with previously reported CdS QDs, which indicates that CdS QDs have been successfully prepared by the method used. The individual absorption spectra of CdS QDs and **DAE 1** in toluene are shown in Fig. 1a.

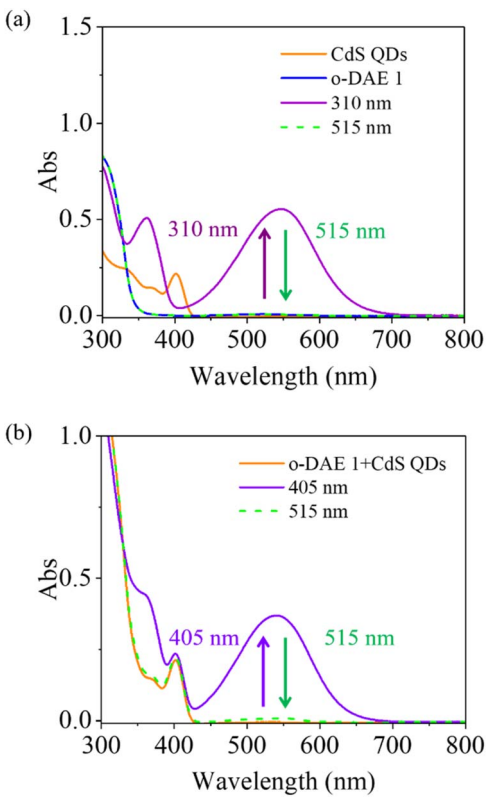

Fig. 1 Absorption spectra of CdS QDs and **DAE 1** responding to light irradiation. (a) Absorption spectra of individual CdS QDs (0.5 μM) and **DAE 1** (50 μM) in toluene. (b) Absorption spectra of the mixture of CdS QDs (0.5 μM) and **DAE 1** (50 μM) in toluene. **DAE 1** was irradiated with 310 nm, 405 nm and 515 nm light to the respective photostationary states.

310 nm (4.5 mW for 16 s) light exposure of the open form of **DAE 1** (o-**DAE 1**, red spectrum) triggers photocyclization to the closed isomer (c-**DAE 1**, blue spectrum), as evidenced by the appearance of the absorption band in the visible region. Subsequent irradiation with 515 nm light (50 mW for 9 min) recovers the initial absorption spectrum as a result of reverse photoisomerization from c-**DAE 1** to o-**DAE 1**. The first absorption peak of CdS QDs was deliberately chosen to be located within the minimal absorption region of both c-**DAE 1** and o-**DAE 1** (here at 405 nm). To confirm the reversible all-visible light photoswitching of our designed system, a mixed solution of CdS QDs (0.5 μM) and **DAE 1** (50 μM), yielding a molar ratio of 1 : 100, was initially irradiated at 405 nm followed by exposure to light at 515 nm. The resulting changes in the absorption spectra are shown in Fig. 1b. Upon 405 nm light irradiation, the appearance of the absorption band centered at 540 nm is a clear testament to the photocyclization from o-**DAE 1** to c-**DAE 1**. Since o-**DAE 1** exhibits negligible absorption at 405 nm, direct photocyclization by this light can be excluded as shown in Fig. S2.† The observed photocyclization results from light absorption by CdS QDs and subsequent TET to o-**DAE 1**, which sensitizes the isomerization to c-**DAE 1**. Further irradiation of the mixed solution with 515 nm light recovers the initial state to 100%. To investigate the reversibility of the mixed solution, the absorbance at 548 nm of the mixed solution is monitored over five irradiation cycles of alternating 405 nm and 515 nm light (Fig. S7a†). For comparison, the sample of only **DAE 1** over five irradiation cycles of alternating 310 nm and 515 nm was measured. Although some fatigue still appears after more than three cycles, it shows improvement compared to under UV light irradiation. We also compare the long-term irradiation stability; two samples were irradiated at 310 nm (only o-**DAE 1**) and 405 nm (CdS QDs + o-**DAE 1**), and the changes in absorbance at 548 nm over 210 s were monitored (Fig. S7b†). It shows that the absorbance of o-**DAE 1** decreased to 87% of its maximum value, while that of the mixed solution only reduced 2% over 210 s, demonstrating the enhanced long-term irradiation stability of our approach (Fig. S7b†).

The reversible process demonstrates that a single CdS QD can achieve reversible photoswitching of multiple **DAE 1** molecules upon exposure to visible light at different wavelengths. It is worth emphasizing that our measurements were conducted under normal atmospheric conditions without excluding oxygen, which simplifies sample preparation and measurements and facilitates further applications.

To gain comprehensive insight into the efficiency of our all-visible light driven system, we investigated four samples with varying molar ratios between CdS QDs and **DAE 1**. The concentration of CdS QDs remained constant at 0.5 μM, whereas the relative ratio of **DAE 1** to CdS QDs was set to 20, 50, 100, and 200. The main photoswitching properties, including the photostationary state (PSS) and photoisomerization quantum yields (QYs), are summarized in Table 1. For ease of comparison, the photochemical properties of also **DAE 1** alone are included in Table 1. Upon direct photocyclization of **DAE 1** using UV light, the PSS consists of 90% c-**DAE 1** and 10% o-**DAE 1**.[16] When CdS QDs were introduced with 20 equivalents of **DAE 1** together with irradiation at 405 nm, an identical conversion rate of 90% c-**DAE 1** and 10% o-**DAE 1** was observed at the PSS. It should be noted that one CdS QD can sensitize the photocyclization of 18 **DAE 1** molecules using this relative ratio. Although the fraction of photoconverted o-**DAE 1** to yield c-**DAE 1** gradually decreases as the relative amount of **DAE 1** in the mixture increases, the absolute number of formed c-**DAE 1** molecules per CdS QD is increased. In the case of CdS QDs and **DAE 1** at a concentration ratio of 1 : 200, a 44% conversion indicates that one CdS QD can isomerize 88 **DAE 1** molecules to the closed form (Table 1). The increased concentration of **DAE 1** in the mixture implies a larger number of molecules actively engaging in dynamic anchoring to the surface of QDs, allowing a single CdS QD to sensitize more DAEs. At the same time, as a larger fraction of **DAE 1** molecules remain free in solution, the overall fraction of **DAE 1** bound to CdS QDs is reduced. Without efficient TET to this fraction, these molecules are more prone to photocycloreversion to yield o-**DAE 1** by direct absorption of the 405 nm light. To underscore the merit of our simple direct mixing approach, a CdS QD-DAE sample was prepared using the ligand exchange method (details in the ESI†). Although the ligand exchange sample also undergoes all-visible light-activated photoswitching as shown in Fig. S3,† the sensitized **DAE 1** molecule per QD in this approach is 9, significantly lower than those achieved through the method of direct mixing.

Table 1 Photoswitching properties of CdS QDs mixed with **DAE 1**

CdS QDs : **DAE 1**	PSS	n^d	$\Phi_{c-o}{}^e$	$\Phi_{o-c}{}^f$
1 : 20	90%[a]	18	0.014[c]	0.20[a]
1 : 50	75%[a]	37	0.011[c]	0.29[a]
1 : 100	61%[a]	61	0.012[c]	0.30[a]
1 : 200	44%[a]	88	0.014[c]	0.34[a]
DAE 1 only	90%[a]		0.012[c]	0.40[b]

[a] Irradiation at 405 nm. [b] Irradiation at 310 nm. [c] Irradiation at 515 nm. [d] The number of c-**DAE 1** formed per CdS QD. [e] Photocycloreversion QYs. [f] Photocyclization QYs.

In order to quantify the efficiency of visible light control, the photoisomerization QYs of **DAE 1** mixed with CdS QDs under 405 nm and 515 nm were determined by using ferrioxalate and Aberchrome 670 actinometers according to previous reports[43–46] (see the ESI† for more details). When the concentration of **DAE 1** in the CdS QD solution increased, the photocyclization QYs of **DAE 1** (Φ_{o-c}) under 405 nm light irradiation improved from 20% (molar ratio 1 : 20) to 34% (molar ratio 1 : 200), approaching that of **DAE 1** alone under direct exposure to 310 nm light (40%). The enhanced Φ_{o-c} is ascribed to the increased TET efficiency as more DAE molecules dynamically attach to the CdS QDs (*vide infra* and Table S1†). However, the energy transfer efficiency no longer improves once **DAE 1** saturates the surface coverage. When the molar ratio of CdS QD/DAE reaches 1 : 400, the lifetime and energy transfer efficiency are identical to those at a 1 : 200 ratio (Table S1†). We also investigated the photocycloreversion QYs of **DAE 1** (Φ_{c-o}) upon 515 nm light irradiation, and it was found that the presence of CdS QDs had no impact on the efficiency of the back conversion from the ring-

closed to the ring-open form of **DAE 1**. This underscores another advantage of the direct mixing approach: it does not affect the ring-opening reaction, which typically is substantially suppressed in previously reported examples relying on covalent attachment and conjugation extension.[39,47,48]

Mechanistic considerations

To gain deeper mechanistic insights into the system, steady-state and time resolved photoluminescence (PL) measurements were performed. The emitting state of semiconductor QDs involves exchange splitting between excited singlets and triplets,[49] facilitating the direct population of molecular triplets *via* energy transfer upon excitation of the QDs.[50] This energy transfer can be evidenced by the observed PL quenching in the QDs.[51] CdS QDs exhibit an emission band with the PL maximum at 425 nm (red curve in Fig. 2a). The PL decay of CdS QDs is multi-exponential with an amplitude-weighted average lifetime of 13.4 ns, as shown by the red curve in Fig. 2b (fitting procedures are described in Fig. S4†). Introducing **DAE 1** into the CdS QD solution leads to significant quenching of both the PL intensity and lifetime as shown in Fig. 2. Remarkably, strong PL quenching occurred even at a molar ratio as low as 1 : 20 between CdS QDs and **DAE 1**, resulting in a significant reduction in the PL intensity and a shortening of the PL lifetime to 0.9 ns (Fig. S4 and Table S1†). The efficiency of the energy transfer (Φ_{ET}) from CdS QDs to **DAE 1** can be estimated to be 93% from both PL intensity quenching and PL lifetime quenching. Φ_{ET} was further enhanced and approached unity when the concentration of **DAE 1** successively increased. This highly efficient energy transfer from CdS QDs to **DAE 1** is key to achieving well-performing visible-light photoswitching in our design. The Stern–Volmer plots of PL intensity and lifetime are shown in Fig. 2c and d and fitted to eqn S11.† The fitting resulted in a high quenching rate constant $k_q = 8.3 \times 10^{13}$ M^{-1} s^{-1}, which is two orders of magnitudes higher than the expected diffusion-controlled rate constant $k_{diff} = 1.1 \times 10^{11}$ M^{-1} s^{-1} in toluene.[28] The high quenching rate constant here is almost as high as that previously reported for CdSe QDs conjugated to organic dyes, $k_q \sim 5 \times 10^{14}$ M^{-1} s^{-1}, where efficient energy transfer occurs between adsorbed dye molecules and the excited CdSe QDs.[52] In our case, the high quenching rate constant results from the close proximity between the core of CdS QDs and **DAE 1** molecules, facilitated by the carboxylic acid functional group of **DAE 1** anchoring to the surface of the CdS QDs. This close proximity, along with the short PL lifetime of CdS QDs (13.4 ns compared to the previously used sensitizer's microsecond and millisecond triplet lifetimes), also explains the insensitivity to oxygen.

Solid-state manipulation

The efficient and oxygen-insensitive all-visible photoswitchable system inspired us to further explore the solid-state

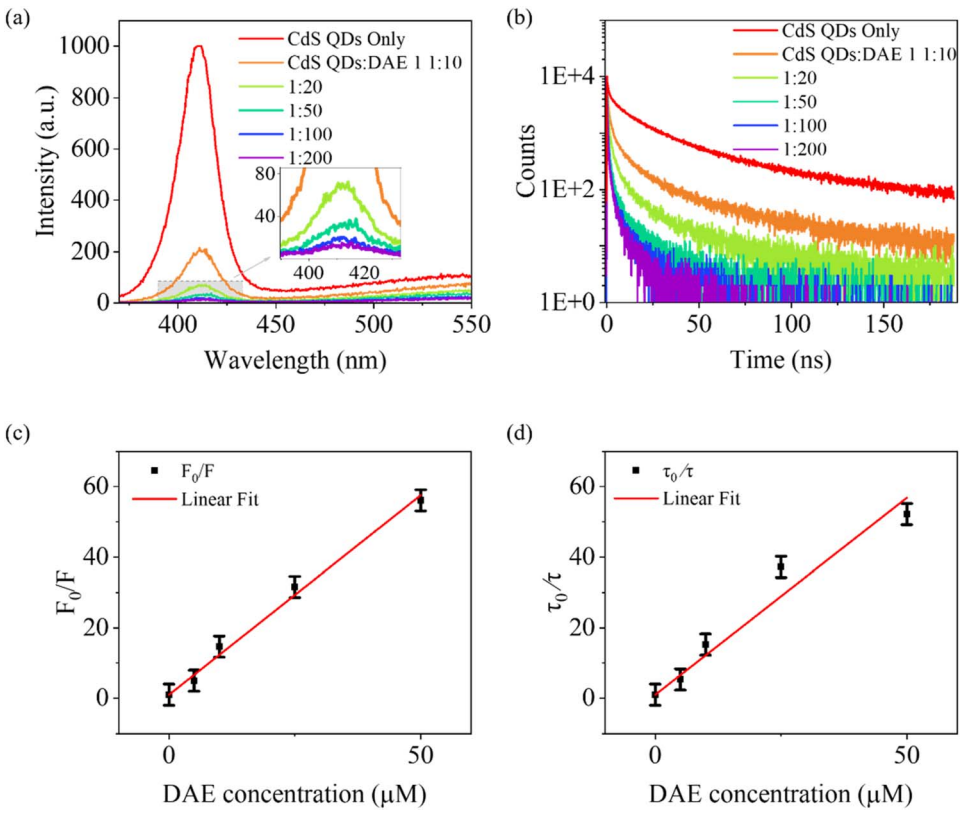

Fig. 2 Photoluminescence and quenching behavior of CdS QDs and **DAE 1**. (a) PL intensity quenching (insets show magnified time-resolved fluorescence quenching in the 390–430 nm range and (b) PL lifetime of the CdS QD emission with and without **DAE 1** (relative concentrations of 10, 20, 50, 100 and 200) in toluene. Stern–Volmer plots and linear fits for (c) the PL intensity and (d) the PL lifetime quenching of CdS QDs.

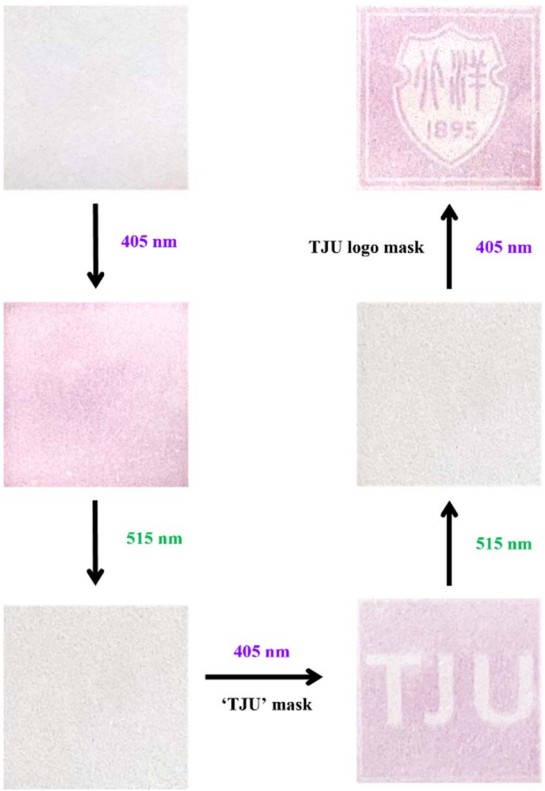

Fig. 3 All-visible-light switching in the solid state. Images of a piece of paper prepared from CdS QDs and DAE 1 solution, and its subsequent color (white and purple) and pattern change ('TJU' and Tianjin University Logo), upon visible light irradiation by altering the wavelength between 405 nm and 515 nm in a normal atmospheric environment.

performance because of the need for deep penetration irradiation in photomodulation devices such as transistors. A solid sample was prepared by depositing CdS QDs (5 μM) and **DAE 1** (1 mM) solution onto a 10 mm × 10 mm filter paper (see the ESI† for details on the sample preparation). This solid sample allowed to reversibly write and erase different patterns through alternating irradiation with 405 nm and 515 nm light, as shown in Fig. 3. Initially, the paper appeared white due to the weak absorption of CdS QDs and o-**DAE 1** in the visible region. When uniformly illuminated with 405 nm light, the entire paper turned a pink-purple hue as a result of the absorption of c-**DAE 1** in the visible region. The color of the paper can be completely faded when exposed to 515 nm light. By employing photomasks, the patterns of 'TJU' and the Tianjin University logo were also written and erased consecutively by simply altering between the two visible wavelengths. This solid-state sample also shows good reversibility over five irradiation cycles of alternating 405 and 515 nm light (Fig. S6†), indicating that the material can be repeatedly used for information encryption. Moreover, this solid-state approach offers good oxygen and fatigue resistance, as it can still undergo conversion upon 405 nm irradiation even after 5 days of exposure to the ambient environment (see Fig. S5†).

Conclusions

In conclusion, we have demonstrated an efficient all-visible light-activated photoswitchable system comprising CdS QDs and carboxylated DAE (**DAE 1**) through a simple non-covalent mixing approach. Upon 405 nm irradiation, **DAE 1** undergoes photocyclization *via* triplet energy transfer from CdS QDs, with PSS and photochemical QYs comparable to those observed under direct UV light irradiation. Due to the high surface area-to-volume ratio and the efficient nature of the light absorption and subsequent TET from CdS QDs to the DAEs, a single CdS QD can sensitize at least 18 **DAE 1** molecules to undergo all-visible light switching, surpassing the performance of previous organic sensitizers and covalent designs. Importantly, the all-visible light switching process of this system is not affected by the presence of oxygen, thanks to the close proximity of the QDs and the DAEs, the short PL lifetime, and the efficient energy transfer process. When adapted to the solid-state, it allows for the reversible writing and erasing of colour patterns within the same sample, even when exposed to the ambient atmosphere. These findings hold the potential to develop all-visible light-activated photoresponsive materials towards smart optoelectronic devices and imaging.

Data availability

All the relevant data are provided as part of the ESI.†

Author contributions

L. H. conceived the concept and supervised the research. L. H. and K. C. designed the project. L. H. and K. C. carried out material synthesis. K. C. and J. L. performed material characterization tests. K. Z., L. H., and B. A. wrote the paper. T. L. provided advice on the research. All authors discussed the results and commented on the manuscript.

Conflicts of interest

There are no conflicts to declare.

Acknowledgements

L. H. acknowledges support from the National Key Research and Development Project of China (2023YFB3609300) and National Natural Science Foundation of China (62205240 and 12274320), and L. H. and B. A. acknowledge support from the Swedish Foundation for International Cooperation in Research and Higher Education (STINT IB2023-9189). We thank Dr Shiming Li for providing DAE.

Notes and references

1 S. Kundu, A. Chowdhury, S. Nandi, K. Bhattacharyya and A. Patra, *Chem. Sci.*, 2021, **12**, 5874–5882.
2 J. Zhang, Y. Fu, H. H. Han, Y. Zang, J. Li, X. P. He, B. L. Feringa and H. Tian, *Nat. Commun.*, 2017, **8**, 987.

3 H. B. Cheng, S. Zhang, E. Bai, X. Cao, J. Wang, J. Qi, J. Liu, J. Zhao, L. Zhang and J. Yoon, *Adv. Mater.*, 2022, **34**, e2108289.
4 Z. Zhang, W. Wang, M. O'Hagan, J. Dai, J. Zhang and H. Tian, *Angew. Chem., Int. Ed.*, 2022, **61**, e202205758.
5 N. Hosono, M. Yoshikawa, H. Furukawa, K. Totani, K. Yamada, T. Watanabe and K. Horie, *Macromolecules*, 2013, **46**, 1017–1026.
6 A. Goulet-Hanssens, T. C. Corkery, A. Priimagi and C. J. Barrett, *J. Mater. Chem. C*, 2014, **2**, 7505–7512.
7 J. Gemen, J. R. Church, T. P. Ruoko, N. Durandin, M. J. Bialek, M. Weissenfels, M. Feller, M. Kazes, M. Odaybat, V. A. Borin, *et al.*, *Science*, 2023, **381**, 1357–1363.
8 J. Zhang and H. Tian, *Adv. Opt. Mater.*, 2018, **6**, 1701278.
9 M. Irie, T. Fukaminato, K. Matsuda and S. Kobatake, *Chem. Rev.*, 2014, **114**, 12174–12277.
10 M. Irie, T. Fukaminato, T. Sasaki, N. Tamai and T. Kawai, *Nature*, 2002, **420**, 759–760.
11 V. Lemieux and N. R. Branda, *Org. Lett.*, 2005, **7**, 2969–2972.
12 U. Al-Atar, R. Fernandes, B. Johnsen, D. Baillie and N. R. Branda, *J. Am. Chem. Soc.*, 2009, **131**, 15966–15967.
13 K. Uchida, M. Saito, A. Murakami, S. Nakamura and M. Irie, *ChemPhysChem*, 2003, **4**, 1124–1127.
14 G. Naren, W. Larsson, C. Benitez-Martin, S. Li, E. Perez-Inestrosa, B. Albinsson and J. Andreasson, *Chem. Sci.*, 2021, **12**, 7073–7078.
15 A. A. Scherbovich, S. A. Maskevich, P. V. Karpach, G. T. Vasilyuk, V. I. Stsiapura, O. V. Venidiktova, A. O. Ayt, V. A. Barachevsky, A. A. Khuzin, A. R. Tuktarov, *et al.*, *J. Phys. Chem. C*, 2020, **124**, 27064–27070.
16 L. Hou, R. Ringstrom, A. B. Maurer, M. Abrahamsson, J. Andreasson and B. Albinsson, *J. Am. Chem. Soc.*, 2022, **144**, 17758–17762.
17 S. A. Diaz, F. Gillanders, E. A. Jares-Erijman and T. M. Jovin, *Nat. Commun.*, 2015, **6**, 6036.
18 D. Mendive-Tapia, A. Perrier, M. J. Bearpark, M. A. Robb, B. Lasorne and D. Jacquemin, *Phys. Chem. Chem. Phys.*, 2014, **16**, 18463–18471.
19 D. Bleger and S. Hecht, *Angew. Chem., Int. Ed.*, 2015, **54**, 11338–11349.
20 Z. Xu, T. Jin, Y. Huang, K. Mulla, F. A. Evangelista, E. Egap and T. Lian, *Chem. Sci.*, 2019, **10**, 6120–6124.
21 Z. Zhang, J. Zhang, B. Wu, X. Li, Y. Chen, J. Huang, L. Zhu and H. Tian, *Adv. Opt. Mater.*, 2018, **6**, 1700847.
22 J. Ma, X. Cui, F. Wang, X. Wu, J. Zhao and X. Li, *J. Org. Chem.*, 2014, **79**, 10855–10866.
23 V. W. Yam, C. C. Ko and N. Zhu, *J. Am. Chem. Soc.*, 2004, **126**, 12734–12735.
24 Z. Zhang, W. Wang, P. Jin, J. Xue, L. Sun, J. Huang, J. Zhang and H. Tian, *Nat. Commun.*, 2019, **10**, 4232.
25 Z. Li, C. He, Z. Lu, P. Li and Y.-P. Zhu, *Dyes Pigm.*, 2020, **182**, 108623.
26 M. Herder, B. M. Schmidt, L. Grubert, M. Patzel, J. Schwarz and S. Hecht, *J. Am. Chem. Soc.*, 2015, **137**, 2738–2747.
27 R. Murata, T. Yago and M. Wakasa, *J. Phys. Chem. A*, 2015, **119**, 11138–11145.
28 M. Montalti and S. L. Murov, *Handbook of photochemistry*, CRC/Taylor & Francis, 2006.
29 R. Murata, T. Yago and M. Wakasa, *Bull. Chem. Soc. Jpn.*, 2011, **84**, 1336–1338.
30 M. T. Indelli, S. Carli, M. Ghirotti, C. Chiorboli, M. Ravaglia, M. Garavelli and F. Scandola, *J. Am. Chem. Soc.*, 2008, **130**, 7286–7299.
31 S. Fredrich, R. Gostl, M. Herder, L. Grubert and S. Hecht, *Angew. Chem., Int. Ed.*, 2016, **55**, 1208.
32 W. Wang, W. Yang, Z. Zhang, J. Dai, Y. Xu and J. Zhang, *Chem. Sci.*, 2024, **15**, 5539–5547.
33 M. Liu, P. Xia, G. Zhao, C. Nie, K. Gao, S. He, L. Wang and K. Wu, *Angew. Chem., Int. Ed.*, 2022, **61**, e202208241.
34 L. Hou, W. Larsson, S. Hecht, J. Andréasson and B. Albinsson, *J. Mater. Chem. C*, 2022, **10**, 15833–15842.
35 K. Taruno, I. Ikariko, T. Taniguchi, S. Kim and T. Fukaminato, *J. Phys. Chem. B*, 2024, **128**, 273–279.
36 P. Hong, J. Liu, K. X. Qin, R. Tian, L. Y. Peng, Y. S. Su, Z. Gan, X. X. Yu, L. Ye, M. Q. Zhu, *et al.*, *Angew. Chem., Int. Ed.*, 2023, **63**, e202316706.
37 T. Fukaminato, T. Doi, M. Tanaka and M. Irie, *J. Phys. Chem. C*, 2009, **113**, 11623–11627.
38 R. T. Jukes, V. Adamo, F. Hartl, P. Belser and L. De Cola, *Inorg. Chem.*, 2004, **43**, 2779–2792.
39 T. Fukaminato, T. Hirose, T. Doi, M. Hazama, K. Matsuda and M. Irie, *J. Am. Chem. Soc.*, 2014, **136**, 17145–17154.
40 S. Qiu, A. T. Frawley, K. G. Leslie and H. L. Anderson, *Chem. Sci.*, 2023, **14**, 9123–9135.
41 Z. Li, Y. Ji, R. Xie, S. Y. Grisham and X. Peng, *J. Am. Chem. Soc.*, 2011, **133**, 17248–17256.
42 W. W. Yu and X. Peng, *Angew. Chem., Int. Ed.*, 2002, **41**, 2368–2371.
43 F. Gillanders, L. Giordano, S. A. Diaz, T. M. Jovin and E. A. Jares-Erijman, *Photochem. Photobiol. Sci.*, 2014, **13**, 603–612.
44 A. P. Glaze, H. G. Heller and J. Whittall, *J. Chem. Soc., Perkin Trans. 2*, 1992, 591–594.
45 K. Shibata, K. Muto, S. Kobatake and M. Irie, *J. Phys. Chem. A*, 2001, **106**, 209–214.
46 T. Sumi, Y. Takagi, A. Yagi, M. Morimoto and M. Irie, *Chem. Commun.*, 2014, **50**, 3928–3930.
47 A. Osuka, D. Fujikane, H. Shinmori, S. Kobatake and M. Irie, *J. Org. Chem.*, 2001, **66**, 3913–3923.
48 F. Hu, M. Cao, X. Ma, S. H. Liu and J. Yin, *J. Org. Chem.*, 2015, **80**, 7830–7835.
49 M. Nirmal and L. Brus, *Acc. Chem. Res.*, 1998, **32**, 407–414.
50 C. Mongin, S. Garakyaraghi, N. Razgoniaeva, M. Zamkov and F. N. Castellano, *Science*, 2016, **351**, 369–372.
51 L. Hou, A. Olesund, S. Thurakkal, X. Zhang and B. Albinsson, *Adv. Funct. Mater.*, 2021, **31**, 2106198.
52 A. M. Funston, J. J. Jasieniak and P. Mulvaney, *Adv. Mater.*, 2008, **20**, 4274–4280.